

See discussions, stats, and author profiles for this publication at: <https://www.researchgate.net/publication/244460247>

Bis(trimethylsilyl)ethyne as a Two-Electron Alkyne Ligand in Group 6 Carbonylmetal(o) Complexes: Photochemical Syntheses and Comprehensive Characterization of $M(CO)_5(\eta^2 Me_3SiC\equiv CMe)_2$

ARTICLE in ORGANOMETALLICS · SEPTEMBER 2005

Impact Factor: 4.13 · DOI: 10.1021/om058016r

CITATIONS

7

READS

159

6 AUTHORS, INCLUDING:



Saim Özkar

Middle East Technical University

298 PUBLICATIONS 5,265 CITATIONS

SEE PROFILE



S. Saldamli

4 PUBLICATIONS 14 CITATIONS

SEE PROFILE

Bis(trimethylsilyl)ethyne as a Two-Electron Alkyne Ligand in Group 6 Carbonylmetal(0) Complexes: Photochemical Syntheses and Comprehensive Characterization of $M(CO)_5(\eta^2\text{-Me}_3\text{SiC}\equiv\text{CSiMe}_3)$ ($M = \text{W}, \text{Mo}, \text{Cr}$) and $\text{trans-Mo}(CO)_4(\eta^2\text{-Me}_3\text{SiC}\equiv\text{CSiMe}_3)_2$

Friedrich-Wilhelm Grevels* and Jürgen Jacke

Max-Planck-Institut für Bioanorganische Chemie (formerly MPI für Strahlenchemie),
Stiftstrasse 34-36, Postfach 10 13 65, D-45413 Mülheim an der Ruhr, Germany

Richard Goddard and Christian W. Lehmann

Max-Planck-Institut für Kohlenforschung, Kaiser-Wilhelm-Platz 1,
D-45470 Mülheim an der Ruhr, Germany

Saim Özkar* and Saltuk Saldamli

Department of Chemistry, Middle East Technical University, 06531 Ankara, Turkey

Received March 31, 2005

Continued irradiation of $\text{W}(CO)_6$ in the presence of excess bis(trimethylsilyl)ethyne (btmse) in *n*-hexane solution yields $\text{W}(CO)_5(\eta^2\text{-btmse})$ as the sole product, with quantum yields of 0.66 and 0.69 at $\lambda_{\text{exc}} = 365$ and 313 nm, respectively. $\text{Cr}(CO)_6$ behaves analogously, while with $\text{Mo}(CO)_6$ the initially generated $\text{Mo}(CO)_5(\eta^2\text{-btmse})$ undergoes further CO substitution to form $\text{trans-Mo}(CO)_4(\eta^2\text{-btmse})_2$ as the second product. All four compounds were isolated in crystalline form and fully characterized by elemental analysis, MS, IR, and NMR spectroscopies as well as by single-crystal X-ray crystallography. They assume a quasi-octahedral coordination geometry with the alkyne triple bond being eclipsed to one OC–M–CO axis and, in the case of $\text{trans-Mo}(CO)_4(\eta^2\text{-btmse})_2$, in *trans*-orthogonal orientation to the second alkyne. Both $\text{Mo}(CO)_5(\eta^2\text{-btmse})$ and $\text{Cr}(CO)_5(\eta^2\text{-btmse})$ are labile toward alkyne displacement by CO, whereas $\text{W}(CO)_5(\eta^2\text{-btmse})$ and $\text{trans-Mo}(CO)_4(\eta^2\text{-btmse})_2$ undergo spontaneous $^{12}\text{CO}/^{13}\text{CO}$ exchange in the dark under mild conditions. Partially ^{13}CO labeled samples generated in this way provide complementary CO stretching vibrational data needed for thorough analyses at the level of the energy-factored CO force field approximation. From all the structural features and spectroscopic data it is evident that bis(trimethylsilyl)ethyne acts as a two-electron donor ligand in this series of d^6 carbonylmetal(0) complexes.

Introduction

The chemistry of group 6 metal(0)-alkyne complexes¹ involves a broad spectrum of alkynes, $\text{R}-\text{C}\equiv\text{C}-\text{R}'$, with properties ranging from very electron poor at one end to electron rich at the other ($\text{R/R}' = \text{CF}_3, \text{CO}_2\text{Me}$, aryl, H, alkyl, SMe, SiMe₃). A variety of structures providing four, five, and six coordination sites are known, which accommodate up to three alkynes along with CO and/or other auxiliary ligands L. This multiformity arises from the presence of the two orthogonal π systems, $\pi_{\parallel}/\pi_{\parallel}^*$ and $\pi_{\perp}/\pi_{\perp}^*$, which make the $-\text{C}\equiv\text{C}-$ unit a rather flexible ligand, capable of using up to four electrons for combined $\sigma(\pi_{\parallel})$ -donor/ $\pi(\pi_{\parallel}^*)$ -acceptor and $\pi(\pi_{\perp})$ -donor/ $\delta(\pi_{\perp}^*)$ -acceptor interaction with a metal center if circumstances permit.²

Particularly well documented are four-coordinate compounds of the general formula $M(CO/L)(\eta^2\text{-R}-\text{C}\equiv\text{C}-\text{R}')_3$ ($M = \text{W},^{3-23} \text{Mo},^{5,8-10,24-29} \text{Cr}^{14,30,31}$). The symmetry of this type of complex (essentially C_{3v} , as initially

(2) For possible problems associated with the “four-electron donor” terminology in the context of suggesting global properties of metal alkyne complexes see: Templeton, J. L. *Adv. Organomet. Chem.* **1989**, 29, 1–100.

(3) Tate, D. P.; Augl, J. M. *J. Am. Chem. Soc.* **1963**, 85, 2174–2175.

(4) Tate, D. P.; Augl, J. M.; Ritchey, W. M.; Ross, B. L.; Grasselli, J. G. *J. Am. Chem. Soc.* **1964**, 86, 3261–3265.

(5) Strohmeier, W.; von Hobe, D. Z. *Naturforsch. B* **1964**, 19, 959–960.

(6) King, R. B.; Fronzaglia, A. *Inorg. Chem.* **1966**, 5, 1837–1846.

(7) Laine, R. M.; Moriarty, R. E.; Bau, R. *J. Am. Chem. Soc.* **1972**, 94, 1402–1403.

(8) Connor, J. A.; Hudson, G. A. *J. Organomet. Chem.* **1975**, 97, C43–C45.

(9) Nesmeyanov, A. N.; Krivykh, V. V.; Kaganovich, V. S.; Rybinskaya, M. I. *J. Organomet. Chem.* **1975**, 102, 185–193.

(10) Connor, J. A.; Hudson, G. A. *J. Organomet. Chem.* **1978**, 160, 159–164.

(11) Odell, K. J.; Hyde, E. M.; Shaw, B. L.; Shepherd, I. J. *Organomet. Chem.* **1979**, 168, 103–114.

(12) Connor, J. A.; Hudson, G. A. *J. Organomet. Chem.* **1980**, 185, 385–390.

* To whom correspondence should be addressed. E-mail: (F.-W.G.) grevels@mpi-muelheim.mpg.de; (S. Ö.) sozkar@metu.edu.tr.

(1) For a brief survey see: Whiteley, M. W. In *Comprehensive Organometallic Chemistry II*; Abel, E. W., Stone, F. G., Wilkinson, G., Eds.; Pergamon: Oxford, U.K., 1995; Vol. 5, Chapter 6.8, pp 363–364.

proposed^{3,4} and later verified by means of X-ray diffraction studies^{7,13,14,18,19,21–23,26–30} dictates that one of the three π_{\perp} orbital combinations remains nonbonding,^{4,32,33} such that the three alkyne ligands jointly supply 10 electrons to the zerovalent d⁶ metal center. Partial utilization of the $\pi(\pi_{\perp})$ alkyne donor capacity also occurs in some five-coordinate complexes containing two alkyne ligands,^{12,18–20,34–37} which apparently contribute an average number of three electrons. Donation of all four electrons to a d⁶ metal(0) center is put into effect by the two alkynes in $\text{Cr}(\text{CO})_2(\eta^2\text{-Me}_3\text{Si-C}\equiv\text{C-SiMe}_3)_2$ ^{14,38} and other four-coordinate bis-alkyne complexes,^{8,12,14,31,39} as well as by the single alkyne ligand in $\text{Cr}(\text{CO})_2[\text{P}(\text{OMe})_3]_2(\eta^2\text{-R-C}\equiv\text{C-Ph})$ ⁴⁰ and other five-coordinate monoalkyne complexes.^{14,41,42}

Alkynes counted as two-electron donors are found in a variety of $\text{M}(\text{CO})_5(\eta^2\text{-alkyne})$ ($\text{M} = \text{W}$,^{43–51} Mo ,^{43,48,52} Cr ^{48–53}), $\text{M}(\text{CO})_2(\eta^6\text{-arene})(\eta^2\text{-alkyne})$ ($\text{M} = \text{Cr}$,^{54–62}

Mo ⁶¹), $\text{M}(\text{CO})_4(\text{carbene})(\eta^2\text{-alkyne})$ ($\text{M} = \text{W}$,^{63,64} Mo ,⁶⁴ Cr ^{64,65}), $\text{M}(\text{CO})_3(\text{L-L})(\eta^2\text{-alkyne})$ ($\text{M} = \text{W}$),^{66,67} and $\text{M}(\text{CO})_2(\text{L-L/L}_2)(\eta^2\text{-alkyne})_2$ ($\text{M} = \text{W}$,^{67,68} Mo ^{69–71}) type complexes. In these six-coordinate d⁶ metal(0)-alkyne compounds with quasi-octahedral geometry, where a vacant metal d(π) orbital mate for the π_{\perp} electrons is not available, the $\text{-C}\equiv\text{C-}$ unit is constrained to functioning as an alkene-like $\sigma(\pi_{\parallel})$ -donor/ $\pi(\pi_{\parallel}^*)$ -acceptor ligand. The presence of the alkyne π_{\perp} electrons deserves nevertheless attention as a possible source of destabilization due to repulsive interaction with a filled metal d(π) orbital.⁶⁷

Low-temperature photolysis of $\text{M}(\text{CO})_6$ in diethyl ether⁵³ or dichloromethane^{47–49,51} and subsequent treatment of the resulting $\text{M}(\text{CO})_5(\text{solv})$ species with an alkyne proved useful for the formation of $\text{M}(\text{CO})_5(\eta^2\text{-alkyne})$ products. In this way, a few $\text{M}(\text{CO})_5(\eta^2\text{-CH}\equiv\text{CR})$ compounds with terminal alkynes ($\text{M} = \text{Cr}$,⁵³ $\text{R} = \text{CO}_2\text{Me}$; $\text{M} = \text{W}$,⁴⁷ $\text{R} = \text{Ph}$, CO_2Me) could be isolated as analytically pure materials. Direct CO photosubstitution of $\text{M}(\text{CO})_6$ by an alkyne with formation of $\text{M}(\text{CO})_5(\eta^2\text{-R-C}\equiv\text{C-R'})$ ($\text{M} = \text{W}$, Mo ; $\text{R/R'} = \text{H}$, alkyl, aryl, SiMe_3)

(13) Chiu, K. W.; Lyons, D.; Wilkinson, G.; Thornton-Pett, M.; Hursthouse, M. B. *Polyhedron* **1983**, *2*, 803–810.

(14) Wink, D. J., Ph.D. Thesis, Harvard University, 1985.

(15) Okuda, J.; Zimmermann, K. H. *J. Organomet. Chem.* **1990**, *384*, C21–C24.

(16) Yeh, W.-Y.; Ting, C.-S.; Chih, C.-f. *J. Organomet. Chem.* **1991**, *427*, 257–262.

(17) Wink, D. J.; Cooper, N. J. *Organometallics* **1991**, *10*, 494–500.

(18) Yeh, W.-Y.; Ting, C.-S.; Peng, S.-M.; Lee, G.-H. *Organometallics* **1995**, *14*, 1417–1422.

(19) Yeh, W.-Y.; Ting, C.-S.; Chien, S.-M.; Peng, S.-M.; Lee, G.-H. *Inorg. Chim. Acta* **1997**, *255*, 335–342.

(20) Yeh, W.-Y.; Chien, S.-M. *J. Organomet. Chem.* **1997**, *548*, 191–194.

(21) Ku, R.-Z.; Chen, D.-Y.; Lee, G.-H.; Peng, S.-M.; Liu, S.-T. *Angew. Chem.* **1997**, *109*, 2744–2746; *Angew. Chem., Int. Ed. Engl.* **1997**, *36*, 2631–2632.

(22) Yeh, W.-Y.; Peng, S.-M.; Lee, G.-H. *Organometallics* **2002**, *21*, 3058–3061.

(23) Yeh, W.-Y.; Li, C.-I.; Peng, S.-M.; Lee, G.-H. *J. Organomet. Chem.* **2004**, *689*, 105–110.

(24) King, R. B. *J. Organomet. Chem.* **1967**, *8*, 139–148.

(25) Kolshorn, H.; Meier, H.; Müller, E. *Tetrahedron Lett.* **1972**, 1589–1592.

(26) Bowerbank, R.; Green, M.; Kirsch, H. P.; Mortreux, A.; Smart, L. E.; Stone, F. G. A. *J. Chem. Soc., Chem. Commun.* **1977**, 245–246.

(27) Szymańska-Buzar, T.; Głowiak, T. *J. Organomet. Chem.* **1994**, *467*, 223–230.

(28) Hogarth, G.; Pang, J. Y. *J. Organomet. Chem.* **1996**, *515*, 193–203.

(29) Mealli, C.; Masi, D.; Galindo, A.; Pastor, A. *J. Organomet. Chem.* **1998**, *569*, 21–27.

(30) Kolobova, N. E.; Zhvanko, O. S.; Andrianov, V. G.; Karapetyan, A. A.; Struchkov, Yu. T. *Koord. Khim.* **1980**, *6* (9), 1407–1416; *Chem. Abstr.* **1980**, *93*, 872 (93:239590z).

(31) Jolly, P. W.; Zakrzewski, U. *Polyhedron* **1991**, *10*, 1427–1431.

(32) King, R. B. *Inorg. Chem.* **1968**, *7*, 1044–1046.

(33) Wink, D. J.; Creagan, B. T. *Organometallics* **1990**, *9*, 328–334.

(34) Hübel, W.; Merényi, R. *J. Organomet. Chem.* **1964**, *2*, 213–221.

(35) Yeh, W.-Y.; Liu, L.-K. *J. Am. Chem. Soc.* **1992**, *114*, 2267–2269.

(36) Yeh, W.-Y.; Ho, C.-L.; Chiang, M. Y.; Chen, I.-T. *Organometallics* **1997**, *16*, 2698–2708.

(37) Wulff, W. D.; Bax, B. M.; Brandvold, T. A.; Chan, K. S.; Gilbert, A. M.; Hsung, R. P.; Mitchell, J.; Clardy, J. *Organometallics* **1994**, *13*, 102–126.

(38) Dötz, K. H.; Mühlemeier, J. *Angew. Chem.* **1982**, *94*, 936–937; *Angew. Chem., Int. Ed. Engl.* **1982**, *22*, 929; *Angew. Chem. Suppl.* **1982**, 2023–2029.

(39) Salt, J. E.; Girolami, G. S.; Wilkinson, G.; Motevalli, M.; Thornton-Pett, M.; Hursthouse, M. B. *J. Chem. Soc., Dalton Trans.* **1985**, 685–692.

(40) Wink, D. J.; Creagan, B. T. *J. Am. Chem. Soc.* **1990**, *112*, 8585–8586.

(41) Wink, D. J.; Fox, J. R.; Cooper, J. N. *J. Am. Chem. Soc.* **1985**, *107*, 5012–5014.

(42) Ishino, H.; Kuwata, S.; Ishii, Y.; Hidai, M. *Organometallics* **2001**, *20*, 13–15.

(43) Stolz, I. W.; Dobson, G. R.; Sheline, R. K. *Inorg. Chem.* **1963**, *2*, 1264–1267.

(44) Landon, S. J.; Shulman, P. M.; Geoffroy, G. L. **1985**, *107*, 6739–6740.

(45) Jacke, J. Doctoral Dissertation; Universität Duisburg/MPI für Strahlenchemie, 1989.

(46) Szymańska-Buzar, T.; Downs, A. J.; Greene, T. M.; Marshall, A. S. *J. Organomet. Chem.* **1995**, *495*, 163–175.

(47) Fischer, H.; Volkland, H.-P.; Früh, A.; Stumpf, J. *Organomet. Chem.* **1995**, *491*, 267–273.

(48) Abd-Elzaher, M. M.; Fischer, H. *J. Organomet. Chem.* **1999**, *588*, 235–241.

(49) Abd-Elzaher, M. M.; Froneck, T.; Roth, G.; Gvozdev, V.; Fischer, H. *J. Organomet. Chem.* **2000**, *599*, 288–297.

(50) Szymańska-Buzar, T.; Kern, K. *J. Organomet. Chem.* **2001**, *622*, 74–83.

(51) Abd-Elzaher, M. M.; Weibert, B.; Fischer, H. *J. Organomet. Chem.* **2003**, *669*, 6–13.

(52) Szymańska-Buzar, T.; Downs, A. J.; Greene, T. M.; Marshall, A. S. *J. Organomet. Chem.* **1995**, *495*, 149–161.

(53) Berke, H.; Härter, P.; Huttner, G.; Zsolnai, L. *Z. Naturforsch. B* **1981**, *36*, 929–937.

(54) Strohmeier, W.; Hellmann, H. *Chem. Ber.* **1965**, *98*, 1598–1607.

(55) Connelly, N. G.; Johnson, G. A. *J. Organomet. Chem.* **1974**, *77*, 341–344.

(56) Alt, H. G.; Engelhardt, H. E.; Filippou, A. C. *J. Organomet. Chem.* **1988**, *355*, 139–148.

(57) Alt, H. G.; Engelhardt, H. E.; Rogers, R. D.; Abu-Orabi, S. T. *J. Organomet. Chem.* **1989**, *378*, 33–43.

(58) Connelly, N. G.; Orpen, A. G.; Rieger, P. H.; Rieger, P. H.; Scott, C. J.; Rosair, G. M. *J. Chem. Soc., Chem. Commun.* **1992**, 1293–1295.

(59) Bartlett, I. M.; Connelly, N. G.; Orpen, A. G.; Quayle, M. J.; Rankin, J. C. *Chem. Commun.* **1996**, 2583–2584.

(60) Connelly, N. G.; Geiger, W. E.; Lagunas, M. C.; Metz, B.; Rieger, A. L.; Rieger, P. H.; Shaw, M. J. *J. Am. Chem. Soc.* **1995**, *117*, 12202–12208.

(61) Bartlett, I. M.; Connelly, N. G.; Martin, A. J.; Orpen, A. G.; Paget, T. J.; Rieger, A. L.; Rieger, P. H. *J. Chem. Soc., Dalton Trans.* **1999**, 691–698.

(62) Adams, C. J.; Bartlett, I. M.; Connelly, N. G.; Harding, D. J.; Hayward, O. D.; Martin, A. J.; Orpen, A. G.; Quayle, M. J.; Rieger, P. H. *J. Chem. Soc., Dalton Trans.* **2002**, 4281–4288.

(63) Foley, H. C.; Strubinger, L. M.; Targos, T. S.; Geoffroy, G. L. *J. Am. Chem. Soc.* **1983**, *105*, 3064–3073.

(64) Dötz, K. H.; Schäfer, T.; Kroll, F.; Harms, K. *Angew. Chem.* **1992**, *104*, 1257–1261; *Angew. Chem., Int. Ed. Engl.* **1992**, *31*, 1236–1238.

(65) Hohmann, F.; Siemoneit, S.; Nieger, M.; Kotila, S.; Dötz, K. H. *Chem. Eur. J.* **1997**, *3*, 853–859.

(66) Birdwhistell, K. R.; Burgmayer, S. J. N.; Templeton, J. L. *J. Am. Chem. Soc.* **1983**, *105*, 7789–7790.

(67) Birdwhistell, K. R.; Tonker, T. L.; Templeton, J. L. *J. Am. Chem. Soc.* **1987**, *109*, 1401–1407.

(68) Hsiao, T.-Y.; Kuo, P.-L.; Lai, C.-H.; Cheng, C.-H.; Cheng, C.-Y.; Wang, S.-L. *Organometallics* **1993**, *12*, 1094–1104.

(69) Lain, J. S.; Cheng, C. H.; Cheng, C. Y.; Wang, S. L. *J. Organomet. Chem.* **1990**, *390*, 333–337.

(70) Lai, C. H.; Cheng, C. H.; Cheng, C. Y.; Wang, S. L. *J. Organomet. Chem.* **1991**, *458*, 147–157.

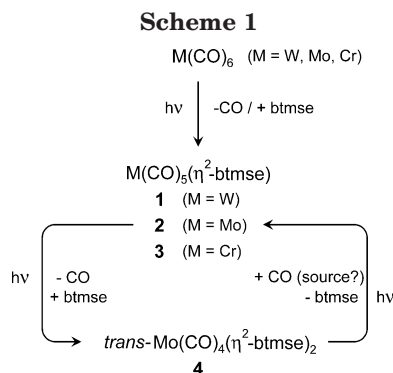
(71) Ardizzoia, G. A.; Brenna, S.; LaMonica, G.; Maspero, A.; Masciocchi, N. *J. Organomet. Chem.* **2002**, *649*, 173–180.

derivatives has been achieved in hydrocarbon solution^{43–45,50} and in low-temperature matrixes as well.^{46,52} With the exception of $\text{W}(\text{CO})_5(\eta^2\text{-btmse})$ [btmse = bis-(trimethylsilyl)ethyne],⁴⁵ none of these compounds could be isolated in pure state, such that the identification rests mainly on the IR $\nu(\text{CO})$ patterns^{43,46,50,52} and NMR data⁵⁰ observed in solution.

The successful use of $\text{W}(\text{CO})_5(\eta^2\text{-btmse})$ (**1**) as a starting material for the preparation of the elusive bisolefin complex $\text{cis-W}(\text{CO})_4(\eta^2\text{-}(E)\text{-cyclooctene})_2$ ⁷² motivated us to examine the photochemical synthesis and properties of **1** in greater detail and to extend these studies to the analogous complexes of molybdenum and chromium.

Results and Discussion

The photoinduced processes occurring upon continued irradiation of hexacarbonyl-tungsten, -molybdenum, or -chromium in the presence of excess bis(trimethylsilyl)ethyne (btmse) are summarized in Scheme 1. In all cases, nearly complete consumption of the starting material can be achieved.



The photoreaction of $\text{W}(\text{CO})_6$ with bis(trimethylsilyl)ethyne affords $\text{W}(\text{CO})_5(\eta^2\text{-btmse})$ (**1**) with isolated yields as high as 80–90%. Multiple CO photosubstitution with formation of, for example, the known tris-alkyne compound $\text{W}(\text{CO})(\eta^2\text{-btmse})_3$ ¹⁷ does not occur. Rather, complex **1** remains the sole product even after prolonged irradiation in the presence of a large excess of bis(trimethylsilyl)ethyne.

This contrasts with observations made with other alkynes. An early IR spectroscopic investigation into the photolysis of $\text{W}(\text{CO})_6$ in the presence of ethyne⁴³ suggests that initially formed $\text{W}(\text{CO})_5(\eta^2\text{-ethyne})$ undergoes secondary CO photosubstitution with formation of $\text{trans-W}(\text{CO})_4(\eta^2\text{-ethyne})_2$. With tolane (diphenylethyne), both thermal and photochemical methods proved successful for converting $\text{W}(\text{CO})_6$ into the $\text{W}(\text{CO})(\eta^2\text{-alkyne})_3$ derivative.⁵ More recently, irradiation of $\text{W}(\text{CO})_6$ in the presence of ethyne and other alkynes, respectively, was claimed to generate mono-, bis-, and tris-alkyne carbonyltungsten species, as concluded from IR and NMR spectra of the resulting reaction mixtures.⁵⁰

Monitoring the photoinduced reaction of $\text{W}(\text{CO})_6$ with bis(trimethylsilyl)ethyne by means of quantitative IR spectroscopy reveals a nearly quantitative material

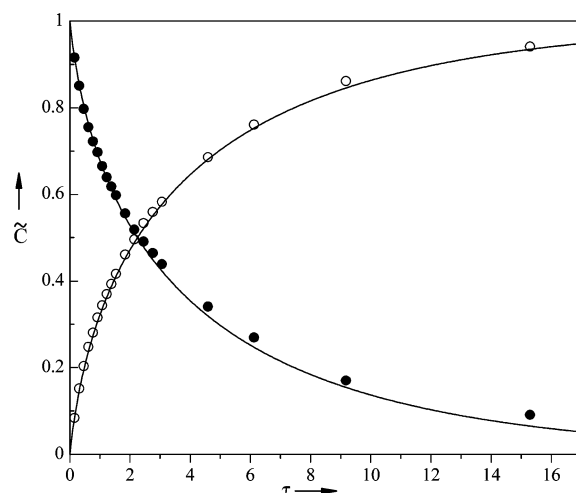


Figure 1. Photochemical conversion of $\text{W}(\text{CO})_6$ (○) into $\text{W}(\text{CO})_5(\eta^2\text{-btmse})$ (**1**, ●) upon irradiation ($\lambda_{\text{exc}} = 365$ nm) in the presence of excess bis(trimethylsilyl)ethyne (btmse) in *n*-hexane solution. The curves represent the functions $\tilde{c} = f(\tau)$ ⁷³ computed with $\Phi = 0.66$, which is determined allowing for internal light filtering by the product,^{74,75} while the symbols indicate the experimental data points from all individual measurements.

balance up to >90% conversion of the starting material into $\text{W}(\text{CO})_5(\eta^2\text{-btmse})$ (**1**). This is illustrated in Figure 1, which shows a plot of the concentrations (\tilde{c})⁷³ of $\text{W}(\text{CO})_6$ and **1** vs the absorbed amount of light (τ)⁷³ for monochromatic irradiation at $\lambda_{\text{exc}} = 365$ nm. The quantum yield, determined with consideration of internal light filtering by the product,^{74,75} is 0.66 at $\lambda_{\text{exc}} = 365$ nm and 0.69 at $\lambda_{\text{exc}} = 313$ nm. These values are in good agreement with the previously reported quantum yield for the analogous conversion of $\text{W}(\text{CO})_6$ into $\text{W}(\text{CO})_5(\eta^2\text{-}(E)\text{-cyclooctene})$,⁷² thus indicating that in either case photolytic loss of CO from $\text{W}(\text{CO})_6$ with formation of $\text{W}(\text{CO})_5(\text{solv})$ is involved as the actual photochemical step.

Analogous reactivity is found for $\text{Cr}(\text{CO})_6$. Upon extended irradiation in the presence of excess bis(trimethylsilyl)ethyne, $\text{Cr}(\text{CO})_5(\eta^2\text{-btmse})$ (**3**) is obtained in about 85% isolated yield. This compound is thermally less stable than the tungsten complex, such that cooling to -25 °C is required during the irradiation and workup of the reaction solution. Here again, no secondary CO photosubstitution takes place, despite the fact that bis(trimethylsilyl)ethyne is known to form $\text{Cr}(\text{CO})_2(\eta^2\text{-btmse})_2$, though via nonphotochemical routes.^{14,38}

Irradiation of $\text{Mo}(\text{CO})_6$ with excess bis(trimethylsilyl)ethyne, in contrast, yields $\text{Mo}(\text{CO})_5(\eta^2\text{-btmse})$ (**2**) along with a second product which is identified as $\text{trans-Mo}(\text{CO})_4(\eta^2\text{-btmse})_2$ (**4**). The formation of **4** is clearly the result of a photoinduced reaction of initially generated

(73) Following our notation in a previous study,⁷² the concentrations of the starting material A and the product B as well as the amount of light absorbed by the system are normalized to the initial concentration of A by setting $\tilde{c}_{A(B)} = c_{A(B)}/c_A^0$ and $\tau = (1/c_A^0) \int_0^t Q_{\text{abs}} dt$.

(74) Kling, O.; Nikolaiski, E.; Schäfer, H. L. *Ber. Bunsen-Ges. Phys. Chem.* **1963**, 67, 883–892.

(75) The evaluation of the quantum yield Φ_{AB} for the photoreaction $A \xrightarrow{h\nu} B$, with consideration of internal light filtering, is based on the functional relationship $\Phi_{AB} = (1/\epsilon_A \tau)[(\epsilon_A - \epsilon_B)(1 - \tilde{c}_A) - \epsilon_B \ln(\tilde{c}_A)]$ (adapted from ref 74) in combination with the stoichiometric condition $\tilde{c}_B = 1 - \tilde{c}_A$. It has been performed by means of a least-squares fit procedure described in footnote 83 of ref 85.

(72) Grevels, F.-W.; Jacke, J.; Klotzbücher, W. E.; Mark, F.; Skibbe, V.; Schaffner, K.; Angermund, K.; Krüger, C.; Lehmann, C. W.; Özkar, S. *Organometallics* **1999**, 18, 3278–3293.

2 (Scheme 1), as verified by a control experiment starting with **2** under the same conditions. However, **2** is not completely converted into **4**, but after some time the conversion ceases. Obviously, the system reaches a photostationary state due to the occurrence of the reverse photoconversion of **4** into **2**. The latter process takes place even in the absence of added CO, as verified by a second control experiment starting with **4** and an excess of the alkyne under argon atmosphere. The origin of the carbon monoxide needed to reconvert the tetracarbonyl complex **4** into the pentacarbonyl complex **2** thus remains unclear.

In solution, both $\text{Mo(CO)}_5(\eta^2\text{-btmse})$ (**2**) and $\text{trans-Mo(CO)}_4(\eta^2\text{-btmse})_2$ (**4**) are only moderately stable, but nevertheless can be isolated from the reaction mixture as analytically pure substances, though with some loss of material in the workup procedure. Therefore, the preparative yields of **2** and **4** are only on the order of 40% and 20%, respectively, even when cooling to -25°C or below is exercised throughout. It is worthy of note that **4** is the first isolated example of a bis-alkyne group 6 metal tetracarbonyl complex.

Characterization of the $\text{M(CO)}_5(\eta^2\text{-btmse})$ Complexes **1, **2**, and **3**.** The structures of all three complexes are collectively displayed in Figure 2; selected distances and angles are listed in Table 1. Essentially, the molecules assume an octahedral arrangement of the six ligands around the metal center with approximate C_{2v} symmetry. The alkyne triple bond is nearly eclipsed to one of the two equatorial OC–M–CO axes of the square-pyramidal M(CO)_5 skeleton. A similar structure was previously found for the phenylethyne complex $\text{W(CO)}_5(\eta^2\text{-HC}\equiv\text{CPh})$.⁴⁷ These findings are in accord with a theoretical study on $\text{W(CO)}_5(\eta^2\text{-acetylene})$,⁷⁶ where the eclipsed structure was predicted to be slightly favored over the staggered one. Compared with free bis(trimethylsilyl)ethyne,⁷⁷ the coordinated $\text{C}\equiv\text{C}$ bond is elongated by about 0.02–0.03 Å. This, together with the remarkable deformation of the Si–C≡C angles (152.9 – 155.6°) from linearity,⁷⁷ is consistent with the notion of a rehybridization of the alkyne carbon atoms from sp toward sp^2 occurring upon coordination.

Perfect C_{2v} symmetry of the M(CO)_5 skeleton would imply that the four equatorial CO ligands are pairwise equivalent, which is indeed more or less the case (Table 1), the difference of about 0.04 Å between the W–C(1) and W–C(3) distances in **1** being the only significant exception. This is likely to be due to crystal packing effects, since the crystal structure of the parent W(CO)_6 shows similar distortions from O_h symmetry (see footnotes 39 and 41 in ref 72). The deviation of the C(1)–M–C(3) angles (164 – 166°) from linearity presumably originates from steric hindrance exerted by the bulky SiMe_3 substituents at the alkyne on the eclipsed carbonyls.

Regarding the unique CO group in *trans*-position to the alkyne, which in all cases shows the shortest M–C and the longest C–O distance (Table 1), the following considerations seem applicable. Recall that, for a pair of CO groups *trans* to each other, only the out-of-phase

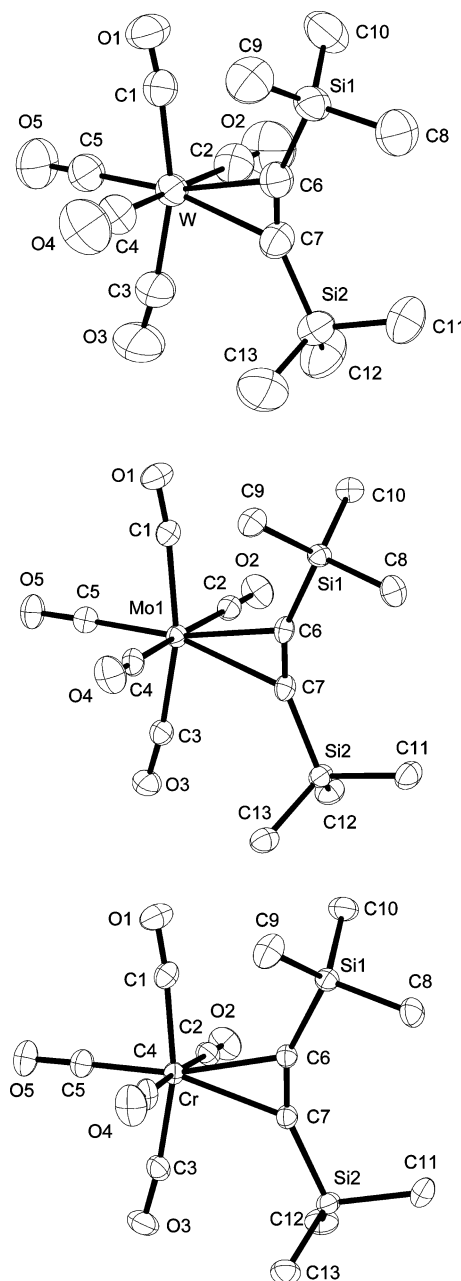


Figure 2. Structures of the $\text{M(CO)}_5(\eta^2\text{-btmse})$ complexes in the crystal. Top: **1**, $\text{M} = \text{W}$. Middle: **2** (one of two crystallographically independent molecules per asymmetric unit), $\text{M} = \text{Mo}$. Bottom: **3**, $\text{M} = \text{Cr}$. Anisotropic displacement ellipsoids shown at the 50% probability level.

combination of the $\text{CO}(\pi^*)$ orbitals has the correct symmetry for interaction with a filled metal $d(\pi)$ orbital. Compared with an individual $\text{CO}(\pi^*)$ orbital, this combination is higher in energy and, hence, interacts less efficiently with the metal $d(\pi)$ orbital. Thus, the unique CO group of the M(CO)_5 units receives more back-donation from the metal than the other four. This in turn makes its M–C bond stronger and its C–O bond weaker, in accord with the observed structural features.

The ^{13}C NMR spectra of the $\text{M(CO)}_5(\eta^2\text{-btmse})$ complexes (Table 2) invariably show, in addition to two resonances associated with the alkyne and methyl carbon atoms of the btmse ligand, two lines for the carbonyl groups in approximately 1:4 intensity ratio. In each case, the signal at lower field is the weaker one and, hence, is assigned to the axial CO (*trans* to the

(76) Pidun, U.; Frenking, G. *J. Organomet. Chem.* **1996**, 525, 269–278.

(77) Bruckmann, J.; Krüger, C. *Acta Crystallogr.* **1997**, C53, 1845–1846.

Table 1. Selected Bond Lengths (Å) and Angles (deg) for W(CO)₅(η²-btmse) (1), Mo(CO)₅(η²-btmse) (2) (only one of the two crystallographically independent molecules per asymmetric unit), and Cr(CO)₅(η²-btmse) (3)

	1	2	3
M–C(1)	2.040(4)	2.053(3)	1.908(2)
M–C(2)	2.070(5)	2.056(3)	1.919(2)
M–C(3)	2.046(5)	2.048(3)	1.902(2)
M–C(4)	2.029(5)	2.066(3)	1.924(2)
M–C(5)	1.980(5)	1.983(3)	1.856(2)
M–C(6)	2.435(4)	2.460(3)	2.363(2)
M–C(7)	2.432(4)	2.465(3)	2.357(2)
C(1)–O(1)	1.142(5)	1.136(3)	1.143(3)
C(2)–O(2)	1.129(6)	1.134(3)	1.136(3)
C(3)–O(3)	1.137(6)	1.143(4)	1.145(3)
C(4)–O(4)	1.137(6)	1.132(3)	1.137(3)
C(5)–O(5)	1.153(5)	1.148(3)	1.146(3)
C(6)–C(7)	1.238(6)	1.227(4)	1.239(3)
C≡C (free btmse): ⁷⁷	1.208(3)		
C(1)–M–C(3)	164.27(17)	164.03(10)	166.02(9)
C(2)–M–C(4)	175.77(17)	174.17(11)	175.93(9)
C(5)–M–C(1)	83.34(17)	82.67(11)	84.01(10)
C(5)–M–C(3)	81.75(19)	81.56(11)	82.01(10)
C(5)–M–C(2)	91.13(19)	92.68(10)	90.11(9)
C(5)–M–C(4)	92.87(19)	92.79(11)	93.94(9)
Si(1)–C(6)–C(7)	154.7(4)	155.6(2)	153.66(17)
Si(2)–C(7)–C(6)	152.9(4)	155.3(2)	154.11(18)
plane[C(6)/M/C(7)]–plane[C(1)/M/C(3)/C(5)]	5.7(4)	6.6(1)	7.8(1)
plane[C(6)/M/C(7)]–plane[C(2)/M/C(4)/C(5)]	87.1(2)	83.5(1)	81.1(1)
plane[C(1)/M/C(3)/C(5)]–plane[C(2)/M/C(4)/C(5)]	89.4(2)	89.6(1)	88.9(2)

Table 2. NMR Chemical Shifts (δ/ppm, in toluene-*d*₆) and IR Data (cm^{−1}, in *n*-hexane) of W(CO)₅(η²-btmse) (1), Mo(CO)₅(η²-btmse) (2), Cr(CO)₅(η²-btmse) (3), *trans*-Mo(CO)₄(η²-btmse)₂ (4), and Free btmse

	1	2 ^a	3 ^a	4	btmse
¹³ C					
≡C–Si	96.3	95.7	90.2	107.9	114.1
Si–CH ₃	0.4	0.1	−0.3	0.2	0.1
CO _{ax}	201.6 ^b	212.1	224.4		
CO _{eq}	198.7 ^c	206.8	218.0	215.0	
¹ H					
Si–CH ₃	0.22	0.17	0.18	0.34	0.02
$\tilde{\nu}$ (CO)					
A ₁ (w)	2080.1	2080.2	2072.9		
A ₁ (vw)	1988.3	1993.9	1988.3	1995.2 (B ₂) ^d	
B ₁ (st)	1960.4	1968.5	1968.7	1968.5 (E) ^d	
B ₂ (st)	1953.0	1956.2	1947.0		
A ₁ (m)	1938.4	1933.5	1932.0		
$\tilde{\nu}$ (C≡C)	1906.0	1943.6	unobserved	1816.3	2107.0

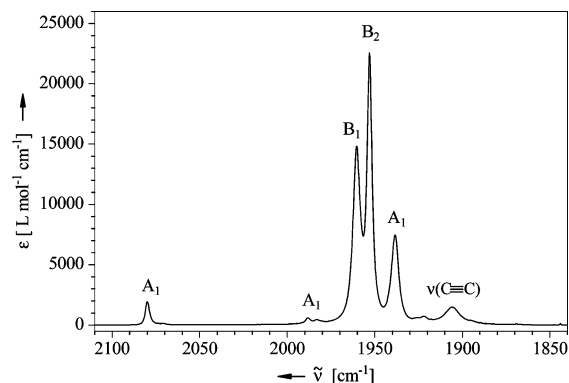
^a IR spectrum recorded in *n*-hexane solution containing 5% free btmse. ^b $J(^{183}\text{W}-^{13}\text{C}) = 148 \text{ Hz}$; $^2J(^{13}\text{C}-^{13}\text{C}) = 3.5 \text{ Hz}$ (from ¹³CO-enriched sample). ^c $J(^{183}\text{W}-^{13}\text{C}) = 124 \text{ Hz}$. ^d Notation according to *D*_{2d} symmetry.

alkyne). The appearance of only one signal for the two pairs of equatorial CO groups indicates that the molecule is fluxional with respect to rotation about the metal–alkyne bond.

The coordination shift of the alkyne carbon atoms to higher field (Δδ 17.8–23.9) corroborates that bis(trimethylsilyl)ethyne functions as a two-electron donor ligand,⁷⁸ by analogy with its behavior in, for example, the molybdenum complex Mo(CO)₂(η⁶-mesitylene)-(η²-btmse)⁶¹ (δ 93.5). By contrast, substantial coordination shifts to lower field have been reported for Cr(CO)₂-(η²-btmse)₂³⁸ (δ 197.8), where btmse functions as a four-electron donor,² and W(CO)₂(η²-btmse)₃¹⁷ (δ 200.7), where the three btmse units donate a total of 10 electrons.

(78) Templeton, J. L.; Ward, B. C. *J. Am. Chem. Soc.* **1980**, *102*, 3288–3290.

The IR spectrum of **1** in the 2100–1850 cm^{−1} region (Figure 3, Table 2) shows, in addition to the ν(CO) modes, a weak feature at 1906 cm^{−1} attributed to the C≡C stretching vibration. The remarkable shift to lower frequency, compared with the free bis(trimethylsilyl)ethyne molecule (2107 cm^{−1}),⁷⁹ goes along with the elongation of the C≡C distance and, thus, is a further indication of the weakening of this bond upon coordination (Table 1).

**Figure 3.** Part of the IR spectrum of W(CO)₅(η²-btmse) (1), recorded in *n*-hexane, showing the ν(CO) bands (2080.1 cm^{−1}/I = 69 km·mol^{−1}, A₁; 1988.3/17, A₁; 1960.4/920, B₁; 1953.0/1030, B₂; 1938.4/430, A₁) and the ν(C≡C) band (1906.0 cm^{−1}/I = 156 km·mol^{−1}).

The appearance of five ν(CO) absorptions, instead of the typical three-band pattern commonly observed in the IR spectra of M(CO)₅L complexes with (local) C_{4v} symmetry (2 A₁, E),^{80–83} clearly reflects the reduction

(79) Doppelt, P.; Baum, T. H. *J. Organomet. Chem.* **1996**, *517*, 53–62.

(80) Cotton, F. A.; Kraihanzel, C. S. *J. Am. Chem. Soc.* **1962**, *84*, 4432–4438.

(81) Kraihanzel, C. S.; Cotton, F. A. *Inorg. Chem.* **1963**, *2*, 533–540.

(82) Haas, H.; Sheline, R. K. *J. Chem. Phys.* **1967**, *47*, 2996–3021.

(83) Braterman, P. S. *Metal Carbonyl Spectra*; Academic Press: London, 1975.

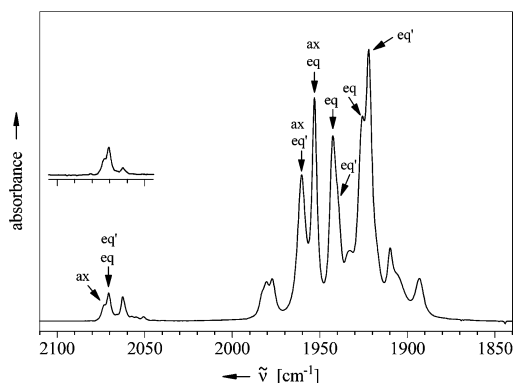


Figure 4. $\nu(\text{CO})$ region in the IR spectrum (recorded in *n*-hexane) of a ^{13}CO -enriched sample of $\text{W}(\text{CO})_5(\eta^2\text{-btmse})$ (**1**) containing 41% **1-1**, 25% **1-2**, and 8% **1-3**. Note that absorptions associated with **1-0** (26%) have been removed by computer-assisted subtraction. Bands marked **ax**, **eq**, and **eq'** refer to the three different stereoisotopomers of **1-1** having the single ^{13}CO group in the axial position (**1-1ax**) or in one of the equatorial positions (**1-1eq**, **1-1eq'**). The inset shows the high-frequency region of a sample with a lower degree of ^{13}CO enrichment (28% **1-1**, 7% **1-2**).

in symmetry to C_{2v} (five IR-active CO stretching modes: 3 A_1 , B_1 , B_2) arising from the single-face π acceptor nature of the alkyne ligand. The two very strong bands in the spectrum shown in Figure 3 (both with intensities of about $1000 \text{ km}\cdot\text{mol}^{-1}$)⁸⁴ are readily assigned to the B_1 and B_2 modes, which correspond to the doubly degenerate E mode under C_{4v} symmetry. One of the A_1 modes is very weak ($17 \text{ km}\cdot\text{mol}^{-1}$), as it corresponds to the IR-inactive B_2 mode under C_{4v} symmetry.

Within the framework of the energy-factored CO force field approximation,^{80–83} the description of the CO stretching modes of the $\text{W}(\text{CO})_5$ unit in **1** involves a total number of eight parameters, viz., three principal force constants, $k(\text{eq})$, $k(\text{eq}')$, and $k(\text{ax})$, along with five interaction constants, $k(\text{eq},\text{eq})$, $k(\text{eq}',\text{eq}')$, $k(\text{eq},\text{eq}')$, $k(\text{eq},\text{ax})$, and $k(\text{eq}',\text{ax})$. Clearly, the five frequencies available from the spectrum of **1** are not sufficient for an analysis, so that additional frequency data from ^{13}CO -enriched samples are needed.

The exchange of ^{12}CO for ^{13}CO in **1** occurs spontaneously in the dark under thermally mild conditions. A sample containing 41% singly labeled $\text{W}(\text{CO})_4(^{13}\text{CO})(\eta^2\text{-btmse})$ (**1-1**), 25% doubly labeled $\text{W}(\text{CO})_3(^{13}\text{CO})_2(\eta^2\text{-btmse})$ (**1-2**), and 8% triply labeled $\text{W}(\text{CO})_2(^{13}\text{CO})_3(\eta^2\text{-btmse})$ (**1-3**) in addition to 26% unlabeled material **1-0** was obtained after 1 h exposure of a *n*-hexane solution of **1** to a ^{13}CO atmosphere at ambient temperature. Computer-assisted removal of the absorptions associated with unlabeled **1-0** from the $\nu(\text{CO})$ spectrum of this sample yields the pattern displayed in Figure 4.

For the singly labeled **1-1**, three stereoisotopomers are possible, $\text{W}(\text{CO})_4(\text{eq-}^{13}\text{CO})(\eta^2\text{-btmse})$ (**1-1eq**), $\text{W}(\text{CO})_4(\text{eq}'\text{-}^{13}\text{CO})(\eta^2\text{-btmse})$ (**1-1eq'**), and $\text{W}(\text{CO})_4(\text{ax-}^{13}\text{CO})(\eta^2\text{-btmse})$ (**1-1ax**), with the ^{13}CO in a *cis*-position (eq or eq') or in the *trans*-position (ax) to the alkyne. The latter one has the same symmetry (C_{2v}) as the unlabeled

complex **1-0**, which implies that the B_1 and B_2 $\nu(\text{CO})$ modes maintain their positions. The former two stereoisotopomers, **1-1eq** and **1-1eq'**, have C_s symmetry with 4 A' and 1 A'' CO stretching vibrations. We have designated the A'' mode of **1-1eq** to be coincident with the B_2 mode of **1-0/1-1ax** and, accordingly, the A'' mode of **1-1eq'** to be coincident with the B_1 mode of **1-0/1-1ax**.

The high-frequency region of the spectrum shown in Figure 4 exhibits two absorptions at 2073.5 and 2070.5 with about 1:4 intensity ratio, together with a third band centered at 2062.4 cm^{-1} . The latter one belongs to the doubly labeled $\text{W}(\text{CO})_3(^{13}\text{CO})_2(\eta^2\text{-btmse})$ (**1-2**), as indicated by its distinctly lower intensity in the spectrum of a sample with a smaller degree of ^{13}CO enrichment (inset in Figure 4). Of the former two absorptions, the one at 2073.5 cm^{-1} is assigned to the axially labeled species **1-1ax**, whereas the corresponding bands of the equatorially labeled isotopomers **1-1eq** and **1-1eq'** appear nearly coincident at 2070.5 cm^{-1} and thus give rise to the higher intensity. The assignment of the bands in the lower frequency region is straightforward on the basis of the above symmetry considerations in combination with the Teller–Redlich product rule,⁸³ absorptions associated with doubly labeled **1-2** again being sorted out by considering intensity changes with increasing ^{13}CO enrichment.

The frequencies of $\text{W}(\text{CO})_5(\eta^2\text{-btmse})$ (**1-0**) and the three stereoisotopomers of $\text{W}(\text{CO})_4(^{13}\text{CO})(\eta^2\text{-btmse})$ (**1-1**) used to determine the energy-factored CO force field parameters are collectively listed in Table 3. The determination is carried out using a previously described program⁸⁵ that fits the calculated frequencies to the observed values in an iterative procedure. In this way, the following results are obtained:

$$\begin{aligned} k(\text{eq}) &= 1604.2 \text{ N}\cdot\text{m}^{-1} & k(\text{eq},\text{eq}) &= 51.6 \text{ N}\cdot\text{m}^{-1} \\ & & k(\text{eq},\text{eq}') &= 29.8 \text{ N}\cdot\text{m}^{-1} \\ k(\text{eq}') &= 1598.9 \text{ N}\cdot\text{m}^{-1} & k(\text{eq}',\text{eq}') &= 58.1 \text{ N}\cdot\text{m}^{-1} \\ & & k(\text{eq},\text{ax}) &= 39.9 \text{ N}\cdot\text{m}^{-1} \\ k(\text{ax}) &= 1547.6 \text{ N}\cdot\text{m}^{-1} & k(\text{eq}',\text{ax}) &= 36.4 \text{ N}\cdot\text{m}^{-1} \end{aligned}$$

The distinctly lower value of $k(\text{ax})$, compared with $k(\text{eq})$ and $k(\text{eq}')$, is consistent with the notion of stronger back-donation to $\text{CO}(\text{ax})$, vide supra. What remains to be discussed is the identity of the CO groups $\text{CO}(\text{eq})$ and $\text{CO}(\text{eq}')$. Taking into account that the carbon monoxide ligands $\text{CO}(1)$ and $\text{CO}(3)$ are eclipsed to the alkyne $\text{C}\equiv\text{C}$ axis (Figure 2), one would expect that the metal $d(\pi) \rightarrow \text{CO}(\pi^*)$ back-donation to these two groups is somewhat diminished due to competitive demand of the alkyne π_{H}^* acceptor orbital for metal $d(\pi)$ electron density, whereas the other two equatorial carbon monoxide ligands $\text{CO}(2)$ and $\text{CO}(4)$ should not be affected in this way. Consequently, the force constants of $\text{CO}(1)$ and $\text{CO}(3)$ should be larger than those of $\text{CO}(2)$ and $\text{CO}(4)$. The ordering $k(\text{eq}) > k(\text{eq}')$ thus identifies $\text{CO}(1)/\text{CO}(3)$ as $\text{CO}(\text{eq})$ and $\text{CO}(2)/\text{CO}(4)$ as $\text{CO}(\text{eq}')$.

Along with the CO force field parameters, the calculation⁸⁵ also yields the eigenvectors connecting the inter-

(84) These values compare well with the integrated intensities of many other metal carbonyls: Noack, K. *Helv. Chim. Acta* **1962**, *45*, 1847–1859.

(85) Footnote 60 in: Grevels, F.-W.; Kerpen, K.; Klotzbücher, W. E.; Schaffner, K.; Goddard, R.; Weimann, B.; Kayran, C.; Özkar, S. *Organometallics* **2001**, *20*, 4775–4792.

Table 3. CO Stretching Frequencies [cm^{-1}] of $\text{W}(\text{CO})_5(\eta^2\text{-btmse})$ (**1-0**) and the Three Stereoisotopomers of $\text{W}(\text{CO})_4(^{13}\text{CO})(\eta^2\text{-btmse})$ (**1-1**)^a

$\text{W}(\text{CO})_5(\eta^2\text{-btmse})$			$\text{W}(\text{CO})_4(^{13}\text{CO})(\eta^2\text{-btmse})$ (1-1)								
1-0			1-1eq			1-1eq'			1-1ax		
C_{2v}	obsd	calcd	C_s	obsd	calcd	C_s	obsd	calcd	C_{2v}	obsd	calcd
A ₁	2080.1	2078.6	A'	2070.5	2071.0	A'	2070.5	2071.1	A ₁	2073.50	2073.9
A ₁	1988.3	1988.3	A'	(~1980)	1982.8	A'	(~1980)	1981.5	A ₁	(~1980)	1988.3
B ₁	1960.4	1960.5				A''	1960.4	1960.5	B ₁	1960.4	1960.5
B ₂	1953.0	1953.0	A''	1953.0	1953.0				B ₂	1953.0	1953.0
A ₁	1938.4	1938.6	A'	1942.4	1942.1	A'	1939.5	1939.7	A ₁	(~1900)	1899.7
			A'	1926.0	1925.7	A'	1921.9	1921.9			

^a Band positions given in parantheses are somewhat uncertain due to overlap with other bands. Consequently, these are not included as input data in the determination of the energy-factored CO force field parameters.

nal CO stretching coordinates r_i with the normal coordinates Q . For the unlabeled parent molecule, $\text{W}(\text{CO})_5(\eta^2\text{-btmse})$ (**1-0**), the following relationships are obtained:

$$Q_1(A_1) = 0.4686(r_1 + r_3) + 0.4642(r_2 + r_4) + 0.3604r_5$$

$$Q_2(A_1) = 0.4894(r_1 + r_3) - 0.5096(r_2 + r_4) + 0.0400r_5$$

$$Q_3(B_1) = 0.7071(r_1 - r_3)$$

$$Q_4(B_2) = 0.7071(r_2 - r_4)$$

$$Q_5(A_1) = 0.2022(r_1 + r_3) + 0.1577(r_2 + r_4) - 0.9319r_5$$

Bearing in mind the nearly square-planar arrangement of the four equatorial CO groups (Figure 2), one can expect that the three A₁ modes gain IR intensity essentially from the contribution of the axial CO stretching (r_5). Accordingly, the low-frequency A₁ mode (Q_5) shows much higher intensity ($430 \text{ km}\cdot\text{mol}^{-1}$) compared with Q_1 ($69 \text{ km}\cdot\text{mol}^{-1}$) and the barely discernible Q_2 ($17 \text{ km}\cdot\text{mol}^{-1}$); see Figure 3.

The $\nu(\text{CO})$ patterns in the IR spectra of $\text{Mo}(\text{CO})_5(\eta^2\text{-btmse})$ (**2**) and $\text{Cr}(\text{CO})_5(\eta^2\text{-btmse})$ (**3**) (Table 2, Figures S-1 and S-2) closely resemble that of the tungsten complex **1**. The only noticeable difference is an increase in the separation of the B₁ and B₂ modes on going from tungsten to molybdenum and chromium. Unfortunately, the alkyne ligand of **2** and **3** is readily displaced by carbon monoxide, which prevents us from preparing ^{13}CO -enriched samples of these two compounds and, hence, from carrying out a thorough energy-factored CO force field analysis.

Regarding the $\text{C}\equiv\text{C}$ stretching vibration, a shift to higher frequency occurs on going from tungsten to molybdenum, thus reflecting a weaker metal–alkyne interaction in accord with the observed decrease in stability. In the spectrum of **2** it appears at 1943.6 cm^{-1} between two of the $\nu(\text{CO})$ absorptions, viz., the low-frequency A₁ and the B₂ bands. In the case of **3**, the $\nu(\text{C}\equiv\text{C})$ mode is unobserved, presumably hidden by one of the intense $\nu(\text{CO})$ absorptions.

Characterization of $\text{trans-Mo}(\text{CO})_4(\eta^2\text{-btmse})_2$ (4**).** X-ray crystallography reveals that the two alkyne ligands occupy *trans* positions in an essentially octahedral coordination geometry (Figure 5, Table 4). They lie

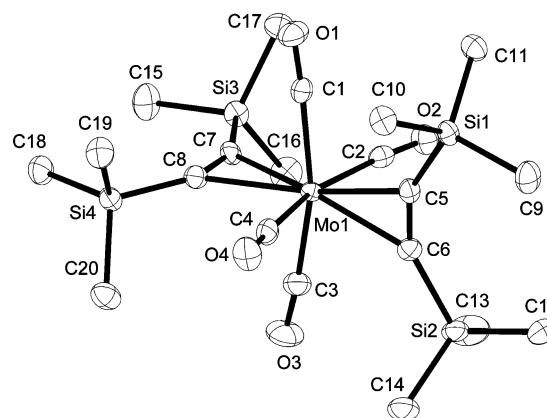


Figure 5. Structure of *trans*- $\text{Mo}(\text{CO})_4(\eta^2\text{-btmse})_2$ (**4**) in the crystal. Note that only one of two crystallographically independent molecules per asymmetric unit is shown. Ellipsoids as in Figure 2.

almost orthogonal to each other (87°) with each alkyne nearly eclipsing one of the two *trans*-OC–Mo–CO units. Closely related structures have been reported for other six-coordinate bis-alkyne group 6 metal(0) complexes,^{67–71} although an example with CO as the sole auxiliary ligand is not yet known.

This type of structure parallels the preferred *trans*-orthogonal orientation of the two olefins in group 6 $\text{M}(\text{CO/L})_4(\eta^2\text{-olefin})_2$ complexes,^{72,86–92} thus underlining that the alkyne does indeed function as an alkene-like two-electron $\sigma(\pi_{\text{H}})$ -donor/ $\pi(\pi_{\text{H}}^*)$ -acceptor ligand. It is a commonly accepted notion that, in this arrangement, two such single-face ligands receive the highest possible π back-donation from a metal(0) center.^{93–95} With this in mind, it is easy to understand why a substantial

(86) Byrne, J. W.; Kress, J. R. M.; Osborn, J. A.; Ricard, L.; Weiss, R. E. *J. Chem. Soc., Chem. Commun.* **1977**, 662–663.

(87) Grevels, F.-W.; Lindemann, M.; Benn, R.; Goddard, R.; Krüger, C. *Z. Naturforsch. B* **1980**, 35, 1298–1309.

(88) Carmona, E.; Marin, J. M.; Poveda, M. L.; Atwood, J. L.; Rogers, R. D.; Wilkinson, G. *Angew. Chem.* **1982**, 94, 467; *Angew. Chem., Int. Ed. Engl.* **1982**, 21, 441.

(89) Carmona, E.; Marin, J. M.; Poveda, M. N.; Atwood, J. L.; Rogers, R. D. *J. Am. Chem. Soc.* **1983**, 105, 3014–3022.

(90) Carmona, E.; Galindo, A.; Poveda, M. N.; Rogers, R. D. *Inorg. Chem.* **1985**, 24, 4033–4039.

(91) Toma, J. M. D. R.; Toma, P. H.; Fanwick, P. E.; Bergstrom, D. E.; Byrn, S. R. *J. Crystallogr. Spectrosc. Res.* **1993**, 23, 41–47.

(92) Szymańska-Buzar, T.; Kern, K.; Downs, A. J.; Greene, T. M.; Morris, L. J.; Parsons, S. *New J. Chem.* **1999**, 23, 407–416.

(93) Albright, T. A.; Burdett, J. K.; Whangbo, M.-H. *Orbital Interactions in Chemistry*; Wiley: New York, 1984; p 286.

(94) Bachmann, C.; Demuynck, J.; Veillard, A. *J. Am. Chem. Soc.* **1978**, 100, 2366–2369.

(95) Albright, T. A.; Hoffmann, R.; Thibault, J. C.; Thorn, D. L. *J. Am. Chem. Soc.* **1979**, 101, 3801–3812.

Table 4. Selected Bond Lengths (Å) and Angles (deg) for *trans*-Mo(CO)₄(η^2 -btmse)₂ (4**) (only for one of the two crystallographically independent molecules per asymmetric unit)**

Mo(1)–C(1)	2.040(4)
Mo(1)–C(2)	2.061(4)
Mo(1)–C(3)	2.051(4)
Mo(1)–C(4)	2.057(4)
Mo(1)–C(5)	2.308(3)
Mo(1)–C(6)	2.307(3)
Mo(1)–C(7)	2.306(3)
Mo(1)–C(8)	2.309(3)
C(1)–O(1)	1.136(4)
C(2)–O(2)	1.135(4)
C(3)–O(3)	1.141(5)
C(4)–O(4)	1.138(4)
C(5)–C(6)	1.271(5)
C(7)–C(8)	1.271(5)
C≡C (free btmse): ⁷⁷	1.208(3)
C(1)–Mo(1)–C(3)	164.25(14)
C(2)–Mo(1)–C(4)	163.30(13)
C(1)–Mo(1)–C(2)	89.68(13)
C(1)–Mo(1)–C(4)	91.41(14)
C(2)–Mo(1)–C(3)	91.74(14)
C(3)–Mo(1)–C(4)	91.71(15)
Si(1)–C(5)–C(6)	148.7(3)
Si(2)–C(6)–C(5)	149.6(3)
Si(3)–C(7)–C(8)	151.4(3)
Si(4)–C(8)–C(7)	149.2(3)
plane[C(5)/Mo(1)/C(6)]	
–plane[C(7)/Mo(1)/C(8)]	87.1(3)
plane[C(1)/Mo(1)/C(3)/D(7,8)]	
–plane[C(2)/Mo(1)/C(4)/D(5,6)]	89.5(2)
plane[C(1)/Mo(1)/C(3)/D(7,8)]	
–plane[C(7)/Mo(1)/C(8)]	89.3(2)
plane[C(2)/Mo(1)/C(4)/D(5,6)]	
–plane[C(5)/Mo(1)/C(6)]	86.8(3)

strengthening of the metal–alkyne bond with concomitant weakening of the C≡C bond occurs on going from Mo(CO)₅(η^2 -btmse) (**2**) to *trans*-Mo(CO)₄(η^2 -btmse)₂ (**4**). In detail, the distances between the metal and the alkyne carbon atoms are drastically shortened by about 0.15 Å from 2.460/2.465 Å in **2** to 2.306–2.309 Å in **4**. At the same time, the C≡C distance increases by about 0.04 Å from 1.227 Å in **2** to 1.271 Å in **4** and, moreover, the deformation of the Si–C≡C angles (148.7–151.4°) from linearity is more pronounced than in **2**.

The ¹³C NMR spectrum of **4** (Table 2) shows one signal for the four equivalent carbonyl groups and one signal each for the alkyne and methyl carbon atoms of the two equivalent btmse ligands. The carbonyl signal (δ 215.0) is at lower field than that of the four equatorial carbonyl groups in **2** (δ 206.8). The alkyne carbon atoms in **4** (δ 107.9), like those in **2** (δ 95.7), show a high-field shift compared with free bis(trimethylsilyl)ethyne (δ 114.1), thus further corroborating that in either type of complex the alkyne acts as a two-electron donor. Noteworthy in this context, species believed to be the *trans*-W(CO)₄(η^2 -alkyne)₂ complexes of propyne and *tert*-butylacetylene were reported in a recent paper⁵⁰ to show ¹³C NMR signals of the acetylenic carbon atoms around δ 150.

The IR spectrum of **4** in *n*-hexane (Figure 6A, Table 2) exhibits a strong ν (CO) band at 1968.5 cm^{−1} together with a weak one at 1995.2 cm^{−1} and a ¹³CO isotope satellite band at 1938.0 cm^{−1}. An additional absorption at 1816.3 cm^{−1} is readily assigned to the C≡C stretching vibration; the substantial low-frequency shift compared with **2** (1943.6 cm^{−1}) is a further indication of the

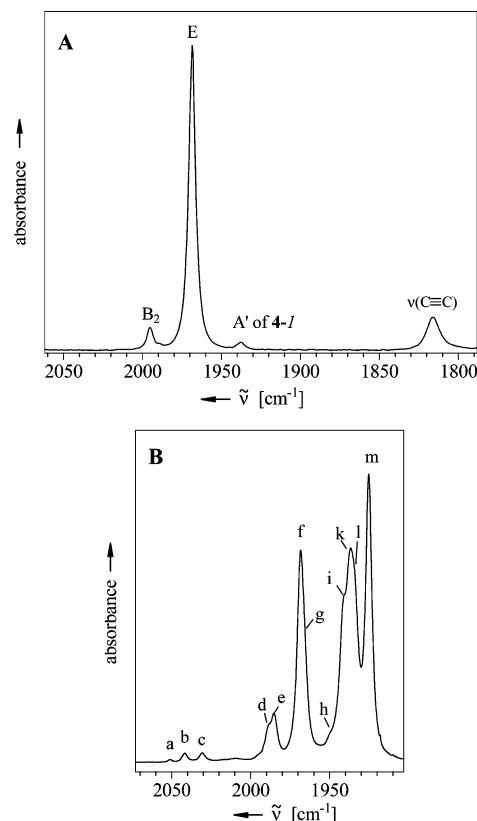


Figure 6. (A) CO stretching vibrational region in the IR spectrum of *trans*-Mo(CO)₄(η^2 -btmse)₂ (**4**) showing two ν (CO) bands at 1995.2 (B₂ of **4-0**) and 1968.5 cm^{−1} (E of **4-0**) along with a ¹³CO isotope satellite band at 1938.0 (A' of **4-1**, present in natural abundance) and the ν (C≡C) absorption at 1816.3 cm^{−1}. (B) Spectrum of a ¹³CO-enriched sample of *trans*-Mo(CO)₄(η^2 -btmse)₂ (**4**) containing **4-1**, **4-2**, and **4-3** in about 1:3:4 ratio, respectively, along with some **4-0** and **4-4**. Both spectra are recorded in *n*-hexane. The band notations in Figure 6B correspond to the assignments in Table 5.

weakening of the C≡C bond on going from **2** to **4**, vide supra.

For *trans*-M(CO)₄L₂ complexes with D_{4h} symmetry, two ν (CO) modes (A_{1g}, B_{2g}) are IR inactive, while a third one, the doubly degenerate E_u CO stretching vibration, is IR active and gives rise to a very strong absorption.⁸³ For the particular case of an M(CO)₄ complex having two single-face ligands in *trans*-orthogonal orientation, such as **4**, the symmetry is reduced to D_{2d}. This does not change the degeneracy of the E_u mode (→ E) and the IR inactivity of A_{1g} mode (→ A₁), but renders the B_{2g} mode IR active (→ B₂). The latter remains nevertheless intrinsically weak as long as the M(CO)₄ moiety does not deviate too far from the square-planar geometry. The structure of **4** meets this condition, as indicated by the *trans*-OC–Mo–CO angles of about 164° (Table 4).

The ν (CO) bands shown in Figure 6A are thus designated as the B₂ and E modes of *trans*-Mo(¹²CO)₄(η^2 -btmse)₂ (**4-0**). The very weak ¹³CO isotope satellite band is attributed to *trans*-Mo(¹²CO)₃(¹³CO)(η^2 -btmse)₂ (**4-1**), present in natural abundance. This species has C_s symmetry, which implies four IR-active CO stretching modes, 3 A' and A'', the latter one being coincident with the E mode of **4-0**. Two of the A' modes of **4-1** are related to the IR-inactive A₁ and the weak B₂ vibrations

Table 5. CO Stretching Frequencies [cm^{-1}] of *trans*-Mo(^{12}CO) $_4(\eta^2\text{-btmse})$ (**4-0**), *trans*-Mo(^{12}CO) $_3(^{13}\text{CO})(\eta^2\text{-btmse})$ (**4-1**), the Two Stereoisotopomers of *trans*-Mo(^{12}CO) $_2(^{13}\text{CO})_2(\eta^2\text{-btmse})$ (**4-2t/4-2c**), *trans*-Mo(^{12}CO) $_3(^{13}\text{CO})(\eta^2\text{-btmse})$ (**4-3**), and *trans*-Mo(^{13}CO) $_4(\eta^2\text{-btmse})$ (**4-4**)^a

4-0			4-1			4-2t		
D_{2d}	obsd ^b	calcd	C_s	obsd	calcd	C_{2v}	obsd	calcd
A ₁	IR inactive	2059.0	A'	2051.2 [a]	2050.9	A ₁	2041.8 [b]	2043.1
B ₂	1995.2 ^b	1995.1	A'	1988.9 [d]	1989.3	B ₁	1968.7 [f]	1968.9
E	1968.5 ^b	1968.9	A''	1968.7 [f]	1968.9	A ₁	1966.3 [g]	1965.6
			A'	1938.0 ^b	1938.0	B ₂	1925.2 [m]	1925.0
4-2c			4-3			4-4		
C_1	obsd	calcd	C_s	obsd	calcd	D_{2d}	obsd	calcd
A	2041.8 [b]	2041.2	A'	2030.7 [c]	2030.5	A ₁	IR inactive	2013.1
A	1985.0 [e]	1985.5	A'	1966.3 [g]	1966.2	B ₂	(~1950, sh) [h]	1950.7
A	1941.5 [i]	1941.6	A'	1937.2 [k]	1936.4			
A	1933.9 [l]	1934.3	A''	1925.2 [m]	1925.0	E	1925.2 [m]	1925.0

^a Lower-case letters in square brackets refer to the band notations in Figure 6B.⁹⁶ ^b Well-resolved maxima in Figure 6A, but barely discernible in Figure 6B.

of **4-0** and, therefore, are intrinsically weak and remain unobserved in this sample. The third one represents the isotopically shifted component of the E mode of **4-0** and, hence, appears with noticeable intensity as the so-called ^{13}CO isotope satellite band.

The D_{2d} structure of **4** implies that three parameters are involved in the description of the CO stretching vibrations within the framework of the energy-factored CO force field approximation, viz., one principal force constant (k) and two interaction constants (k_{cis} and k_{trans}). In principle, these parameters can be evaluated from the combined $\nu(\text{CO})$ data of **4-0** and **4-1** available from the spectrum displayed in Figure 6A. However, for the sake of accuracy we prefer to include additional frequencies from a ^{13}CO -enriched sample. Recall that the fully ^{13}CO -labeled *trans*-Mo(^{13}CO) $_4(\eta^2\text{-btmse})_2$ (**4-4**) does not provide any complementary information, so that partial ^{13}CO enrichment is vital.

The $^{12}\text{CO}/^{13}\text{CO}$ exchange of complex **4** occurs spontaneously in the dark. This is a very fast process, even if the solution is kept at temperatures around 0 °C or below. Therefore, it is difficult to attain the intended partial enrichment, unless the added ^{13}CO is appropriately diluted with argon. A ^{13}CO -enriched sample of **4**, prepared in this way, gives the $\nu(\text{CO})$ IR spectrum displayed in Figure 6B. The assignment of the three weak absorptions in the high-frequency region (marked "a", "b", and "c") to the singly, doubly, and triply ^{13}CO -labeled species **4-1**, **4-2**, and **4-3** is straightforward. They are present in about 1:3:4 ratio, as estimated from the relative intensities of those bands. As regards **4-2**, there exist two stereoisotopomers, **4-2c** and **4-2t**, having the two ^{13}CO groups in *cis* and *trans* position to each other, respectively.

The frequencies and assignments of all bands observed in the two spectra (Figure 6A and 6B)⁹⁶ are collectively listed in Table 5, together with the sym-

metry notations. Bands belonging to the individual isotopomers are grouped with the help of the Teller–Redlich product rule.⁸³ Based on these data sets, the following energy-factored CO force field parameters are obtained by means of the previously described procedure,⁸⁵ which yields an excellent fit of the calculated to the observed frequencies (Table 5).

$$k = 1613.0 \text{ N} \cdot \text{m}^{-1} \quad k_{\text{trans}} = 47.1 \text{ N} \cdot \text{m}^{-1} \\ k_{\text{cis}} = 26.1 \text{ N} \cdot \text{m}^{-1}$$

Conclusions

One might argue that coupling of the $\text{C}\equiv\text{C}$ stretching vibration to the $\nu(\text{CO})$ modes would reduce the quality of the energy-factored CO force field approximation. However, at least for *trans*-Mo(CO) $_4(\eta^2\text{-btmse})_2$ (**4**) the separation in frequency (Table 2) is certainly large enough as to dispel such an objection. Concerning W(CO) $_5(\eta^2\text{-btmse})$ (**1**), which has the lowest $\nu(\text{C}\equiv\text{C})$ frequency among the three M(CO) $_5(\eta^2\text{-btmse})$ complexes, the approximation still seems to work well, as indicated by the satisfactory fit of the calculated to the observed frequencies.

The spontaneous $^{12}\text{CO}/^{13}\text{CO}$ exchange observed for the complex W(CO) $_5(\eta^2\text{-btmse})$ (**1**) parallels the alkyne-facilitated CO substitution observed with group 8 M(CO) $_4(\eta^2\text{-alkyne})$ compounds,⁹⁷ which is thought to involve stabilization of the otherwise unsaturated CO loss species by alkyne $\pi(\pi_{\perp})$ donation in addition to $\sigma(\pi_{\parallel})$ donation.⁹⁸ There is little doubt, if any, that the even faster $^{12}\text{CO}/^{13}\text{CO}$ exchange observed with *trans*-Mo(CO) $_4(\eta^2\text{-btmse})_2$ (**4**) is due to the cooperative effect of the two alkynes.

The facile conversion of **1** into *cis*-W(CO) $_4(\eta^2\text{-(E)-cyclooctene})_2$ ⁷² may also be rationalized in terms of an

(96) Positions of closely spaced bands are located by means of computer-assisted curve fitting using GRAMS/32 (V4.0) software; Galactic Industries Corporation, 395 Main Street, Salem, NH 03079.

(97) Pearson, J.; Cooke, J.; Takats, J.; Jordan, R. B. *J. Am. Chem. Soc.* **1998**, *120*, 1424–1440.

(98) Decker, S. A.; Klobukowski, M. *J. Am. Chem. Soc.* **1998**, *120*, 9342–9355.

alkyne-facilitated CO substitution in the first step, in this case with (*E*)-cyclooctene as the entering ligand, followed by displacement of the alkyne by the second olefin. In this way, relief from the repulsive interaction of the alkyne π_{\perp} electrons with a filled metal $d(\pi)$ is achieved. This would also explain why the alkyne in complexes **2** and **3** is readily displaced by carbon monoxide. Alternatively, an alkyne \rightarrow vinylidene rearrangement could also lead to stabilization, as observed not only with terminal alkynes,^{66,67} but also with bis-(trimethylsilyl)ethyne^{58,61} bound to a group 6 $M(\eta^6\text{-arene})(\text{CO})_2$ unit. In the present study, however, the same alkyne fails to undergo such an isomerization.

Experimental Section

General Remarks. All reactions and manipulations were carried out under argon and in argon-saturated solvents. Photochemical reactions on preparative scale were carried out using a Philips HPK 125-W high-pressure mercury lamp in an immersion-well apparatus⁹⁹ (Solidex glass, $\lambda > 280$ nm), cooled by circulating water or ethanol.

Spectra were recorded on the following instruments: NMR, Bruker Avance DRX 270 (270.1 MHz for ^1H ; 67.9 MHz for ^{13}C) and Bruker Avance DRX 400 (400.1 MHz for ^1H ; 100.6 MHz for ^{13}C); IR, Perkin-Elmer 1600 and Bruker IFS 66, operating with 2 and 0.5 cm^{-1} resolution, respectively; UV-vis, Shimadzu UV-2102 PC; MS, Finnigan MAT 8200. Microanalyses were performed by Mikroanalytisches Laboratorium H. Kolbe, Mülheim an der Ruhr.

Reagents. Analytical grade and deuterated solvents, hexacarbonylchromium(0), hexacarbonylmolybdenum(0), hexacarbonyltungsten(0), and bis(trimethylsilyl)ethyne were purchased from Merck (Darmstadt, Germany) and used as received.

$\text{W}(\text{CO})_5(\eta^2\text{-btmse})$ (1**).** A solution of $\text{W}(\text{CO})_6$ (3.52 g, 10.0 mmol) and bis(trimethylsilyl)ethyne (17.0 g, 100 mmol) in *n*-hexane (400 mL) was irradiated at ambient temperature for 12 h, at which time $\text{W}(\text{CO})_6$ was largely consumed, as monitored by IR spectroscopy. After evaporation of the volatiles (solvent, excess bis(trimethylsilyl)ethyne, and remaining traces of $\text{W}(\text{CO})_6$) in a vacuum (0.1 Pa), the crude product (4.77 g) was recrystallized from *n*-hexane (15 mL) at dry ice temperature to yield yellow crystals of **1**, which were isolated by inverse filtration and dried in a vacuum (4.07 g, 82.4%), mp 68 °C (sealed capillary); a second crop (0.19 g, 3.8%) was obtained from the mother liquor. IR (in *n*-hexane): $\nu(\text{CO}) = 2080.1$ cm^{-1} ($\epsilon = 1920$ $\text{L}\cdot\text{mol}^{-1}\cdot\text{cm}^{-1}$), 1988.3 (605), 1960.4 (14 760), 1953.0 (22 390), 1938.4 (7440); $\nu(\text{C}\equiv\text{C}) = 1906.0$ cm^{-1} ($\epsilon = 1460$ $\text{L}\cdot\text{mol}^{-1}\cdot\text{cm}^{-1}$). UV-vis (*n*-hexane): λ_{max} 237 (56 600), 314 (7490), 375 nm ($\epsilon = 1730$ $\text{L}\cdot\text{mol}^{-1}\cdot\text{cm}^{-1}$). ^1H NMR (toluene-*d*₈): δ 0.22. $^{13}\text{C}\{^1\text{H}\}$ NMR (toluene-*d*₈): δ 201.6, 198.7, 96.3, 0.4. MS: m/z 494 (M^+). Anal. Calcd for $\text{C}_{13}\text{H}_{18}\text{O}_5\text{Si}_2\text{W}$ ($M = 494.30$): C, 31.59; H, 3.67; Si, 11.36; W, 37.19. Found: C, 31.46; H, 3.86; Si, 11.08; W, 35.80.

$\text{Mo}(\text{CO})_5(\eta^2\text{-btmse})$ (2**) and *trans*- $\text{Mo}(\text{CO})_4(\eta^2\text{-btmse})_2$ (**4**).** A solution of $\text{Mo}(\text{CO})_6$ (0.50 g, 1.9 mmol) and bis(trimethylsilyl)ethyne (3.2 g, 18.8 mmol) in *n*-hexane (400 mL) was irradiated at -25 °C for 4.5 h, at which time the progress of product formation ceased as monitored by IR spectroscopy. The residue obtained upon evaporation of the solvent (-40 °C, 0.1 Pa) was chromatographed on silica (Merck Kieselgel 60, 0.063–0.2 mm; column with $l = 30$ cm and $d = 2.5$ cm) at -30 °C with *n*-hexane. As controlled by IR, complex **4** was eluted first, followed by a mixture of complex **2**, unreacted $\text{Mo}(\text{CO})_6$, and bis(trimethylsilyl)ethyne. Removal of the volatiles from the latter mixture in a vacuum (0.1 Pa) at -40 °C, followed by recrystallization from *n*-hexane (35 mL, -40 °C)

at dry ice temperature, yielded pale yellow crystals of **2**, which were isolated by inverse filtration and dried in a vacuum (0.33 g, 43%), mp 47 °C (sealed capillary). IR (in *n*-hexane): $\nu(\text{CO}) = 2080.2$, 1993.9, 1968.5, 1956.2, 1933.5 cm^{-1} ; $\nu(\text{C}\equiv\text{C}) = 1943.6$ cm^{-1} . ^1H NMR (toluene-*d*₈): δ 0.17. $^{13}\text{C}\{^1\text{H}\}$ NMR (toluene-*d*₈): δ 212.1, 206.8, 95.7, 0.1. MS: m/z 408 (M^+). Anal. Calcd for $\text{C}_{13}\text{H}_{18}\text{MoO}_5\text{Si}_2$ ($M = 406.4$): C, 38.42; H, 4.46; Mo, 23.61; Si, 13.82. Found: C, 38.58; H, 4.32; Mo, 23.49; Si, 13.68. The first fraction, upon evaporation to dryness (0.26 g) and recrystallization from *n*-hexane (15 mL, -40 °C) at dry ice temperature, yielded pale yellow crystals of **4** (0.20 g, 19.3%), mp 76 °C (sealed capillary). IR (in *n*-hexane): $\nu(\text{CO}) = 1995.2$, 1968.5 cm^{-1} ; $\nu(\text{C}\equiv\text{C}) = 1816.3$ cm^{-1} . ^1H NMR (toluene-*d*₈): δ 0.34. $^{13}\text{C}\{^1\text{H}\}$ NMR (toluene-*d*₈): δ 215.0, 107.9, 0.2. MS: m/z 550 (M^+). Anal. Calcd for $\text{C}_{20}\text{H}_{36}\text{MoO}_4\text{Si}_4$ ($M = 548.8$): C, 43.77; H, 6.61; Mo, 17.48; Si, 20.47. Found: C, 43.59; H, 6.51; Mo, 17.60; Si, 20.32. Crystals grown from *n*-pentane solution, mp 80 °C (sealed capillary), as used for X-ray diffraction measurements, contain one solvent molecule per two molecules of **4**. Anal. Calcd for $\text{C}_{20}\text{H}_{36}\text{MoO}_4\text{Si}_4\cdot 0.5\text{C}_5\text{H}_{12}$ ($M = 584.9$): C, 46.21; H, 7.24; Mo, 16.40; Si, 19.21. Found: C, 45.84; H, 7.10; Mo, 16.10; Si, 18.69.

$\text{Cr}(\text{CO})_5(\eta^2\text{-btmse})$ (3**).** A solution of $\text{Cr}(\text{CO})_6$ (0.50 g, 2.27 mmol) and bis(trimethylsilyl)ethyne (3.8 g, 22.3 mmol) in *n*-hexane (400 mL) was irradiated at -25 °C for 5 h, at which time $\text{Cr}(\text{CO})_6$ was largely consumed, as monitored by IR spectroscopy. After vacuum evaporation (0.1 Pa) of the volatiles (solvent, excess bis(trimethylsilyl)ethyne, and remaining traces of $\text{Cr}(\text{CO})_6$) at -40 °C, the crude product (0.97 g) was dissolved in *n*-hexane (30 mL, -40 °C) and then cooled to dry ice temperature to yield yellow crystals of **3**, which were isolated by inverse filtration and dried in a vacuum (0.58 g, 70.5%), mp 47 °C (sealed capillary); a second crop (0.13 g, 15.9%) was obtained from the mother liquor. IR: $\nu(\text{CO}) = 2072.9$, 1988.3, 1968.7, 1947.0, 1932.0 cm^{-1} . ^1H NMR (toluene-*d*₈, 223 K): δ 0.18. $^{13}\text{C}\{^1\text{H}\}$ NMR (toluene-*d*₈, 223 K): δ 224.4, 218.0, 90.2, -0.3 . MS: $m/z = 362$ (M^+). Anal. Calcd for $\text{C}_{13}\text{H}_{18}\text{CrO}_5\text{Si}_2$ ($M = 362.4$): C, 43.08; H, 5.01; Cr, 14.34; Si, 15.50. Found: C, 43.03; H, 5.11; Cr, 14.29; Si, 15.36.

^{13}CO Enrichment of $\text{W}(\text{CO})_5(\eta^2\text{-btmse})$ (1**).** A solution of **1** (0.15 g, 0.30 mmol) in *n*-hexane (50 mL) was frozen at liquid nitrogen temperature. After evacuation (0.1 Pa) the solution was allowed to thaw, exposed to 150 mL of ^{13}CO , and stirred for 1 h at rt in the dark. After freezing the solution, carbon monoxide was pumped out. The solution was thawed again, reduced in vacuo to 10 mL, and cooled to dry ice temperature, whereupon yellow crystals precipitated. These were isolated by inverse filtration and dried in vacuo (50 mg). MS: $26 \pm 5\%$ $\text{W}^{(12}\text{CO})_5(\eta^2\text{-btmse})$, $41 \pm 5\%$ $\text{W}^{(12}\text{CO})_4(^{13}\text{CO})(\eta^2\text{-btmse})$, $25 \pm 5\%$ $\text{W}^{(12}\text{CO})_3(^{13}\text{CO})_2(\eta^2\text{-btmse})$, $8 \pm 5\%$ $\text{W}^{(12}\text{CO})_2(^{13}\text{CO})_3(\eta^2\text{-btmse})$. The identity was verified by $^{13}\text{C}\{^1\text{H}\}$ NMR spectroscopy. A sample containing $65 \pm 3\%$ $\text{W}^{(12}\text{CO})_5(\eta^2\text{-btmse})$, $28 \pm 3\%$ $\text{W}^{(12}\text{CO})_4(^{13}\text{CO})(\eta^2\text{-btmse})$, and $7 \pm 3\%$ $\text{W}^{(12}\text{CO})_3(^{13}\text{CO})_2(\eta^2\text{-btmse})$ was analogously prepared, but with exposure to ^{13}CO at 0 °C.

^{13}CO Enrichment of *trans*- $\text{Mo}(\text{CO})_4(\eta^2\text{-btmse})_2$ (4**).** A solution of **4** (0.08 g, 0.16 mmol) in *n*-hexane (100 mL), prepared at -10 °C, was frozen at liquid nitrogen temperature. After evacuation (0.1 Pa) the solution was allowed to thaw at -10 °C, exposed to 16 mL of ^{13}CO (diluted with Ar to 100 mL), and stirred for 10 min in the dark. After freezing the solution, the gas phase was pumped out. The solution was thawed again and evaporated in vacuo to dryness. The residue was recrystallized by dissolving it in 2 mL of *n*-hexane at 0 °C, followed by cooling to dry ice temperature, whereupon pale yellow crystals precipitated. These were isolated by inverse filtration and dried in vacuo (10 mg). The identity was verified by MS and IR spectroscopy, indicating the existence of singly, doubly, and triply ^{13}CO -labeled **4** in about 1:3:4 ratio (see Figure 6B).

Quantum Yield for the Conversion of $\text{W}(\text{CO})_6$ into **1.** Light absorption was measured by means of a modified version

(99) Grevels, F.-W.; Reuvers, J. G. A.; Takats, J. *Inorg. Synth.* **1986**, *24*, 176–180.

Table 6. Details of the X-ray Crystal Structure Analyses for the Complexes $\text{W}(\text{CO})_5(\eta^2\text{-btmse})$ (**1**), $\text{Mo}(\text{CO})_5(\eta^2\text{-btmse})$ (**2**), $\text{Cr}(\text{CO})_5(\eta^2\text{-btmse})$ (**3**), and *trans*- $\text{Mo}(\text{CO})_4(\eta^2\text{-btmse})_2$ (**4**)

	1	2	3	4
formula	$\text{C}_{13}\text{H}_{18}\text{O}_5\text{Si}_2\text{W}$	$\text{C}_{13}\text{H}_{18}\text{O}_5\text{Si}_2\text{Mo}$	$\text{C}_{13}\text{H}_{18}\text{O}_5\text{Si}_2\text{Cr}$	$\text{C}_{20}\text{H}_{36}\text{MoO}_4\text{Si}_4 \cdot 0.5\text{C}_5\text{H}_{12}$
color	yellow	pale yellow	pale yellow	pale yellow
fw, $\text{g}\cdot\text{mol}^{-1}$	494.30	406.39	362.45	584.86
<i>T</i> , K	293	100	100	100
wavelength, Å	0.71069	0.71073	0.71073	0.71073
cryst syst	triclinic	monoclinic	triclinic	monoclinic
space group (no.)	$P\bar{1}$ (no. 2)	$C2/c$ (no. 15)	$P\bar{1}$ (no. 2)	$C2/c$ (no. 15)
<i>a</i> , Å	9.213(1)	12.7653(6)	9.3397(6)	44.9415(19)
<i>b</i> , Å	9.820(1)	14.7293(8)	9.9580(6)	12.5998(5)
<i>c</i> , Å	12.405(1)	30.1204(16)	10.7707(7)	31.8539(14)
α , deg	81.89(1)		103.742(3)	
β , deg	77.16(1)	91.207(3)	106.042(2)	134.841(3)
γ , deg	63.56(1)		95.106(3)	
<i>V</i> , Å ³	978.64(17)	5662.1(5)	922.24(10)	12789.7(9)
<i>Z</i>	2	12	2	16
density(calcd), $\text{Mg}\cdot\text{m}^{-3}$	1.677	1.430	1.305	1.215
abs coeff, mm^{-1}	6.038	0.836	0.764	0.582
<i>F</i> (000), e	476	2472	376	4912
cryst size, mm^3	$0.26 \times 0.18 \times 0.13$	$0.28 \times 0.28 \times 0.14$	$0.42 \times 0.39 \times 0.31$	$0.35 \times 0.35 \times 0.12$
θ range for data collection	1.69 to 29.87°	2.77 to 27.46°	2.05 to 33.84°	1.74 to 33.87°
index ranges	$-12 \leq h \leq 12$ $-13 \leq k \leq 13$ $-15 \leq l \leq 17$	$-11 \leq h \leq 16$ $-13 \leq k \leq 18$ $-39 \leq l \leq 28$	$-14 \leq h \leq 8$ $-15 \leq k \leq 13$ $-13 \leq l \leq 16$	$-57 \leq h \leq 69$ $-16 \leq k \leq 19$ $-47 \leq l \leq 49$
no. of reflns collected	9619	12 565	10 095	69 603
no. of indep reflns	5639	5092	6072	24 157
<i>R</i> _{int}	0.0221	0.0540	0.0195	0.0558
no. of reflns with <i>I</i> > 2σ(<i>I</i>)	4557	4111	5213	18 133
completeness	99.9%	78.4%	81.6%	93.5%
abs corr	Gaussian	psi-scan	empirical	Gaussian
max. and min. transmn	0.71 and 0.52	0.56 and 0.52	0.85 and 0.57	0.94 and 0.82
no. of data/restraints/params	5639/0/190	5092/0/286	6072/0/190	24 157/0/568
goodness-of-fit on <i>F</i> ²	1.050	1.051	1.143	1.233
final <i>R</i> indices [<i>I</i> > 2σ(<i>I</i>)]	<i>R</i> ₁ = 0.0311	<i>R</i> ₁ = 0.0320	<i>R</i> ₁ = 0.0420	<i>R</i> ₁ = 0.0644
<i>R</i> indices (all data)	<i>wR</i> ₂ = 0.0749	<i>wR</i> ₂ = 0.0823	<i>wR</i> ₂ = 0.1283	<i>wR</i> ₂ = 0.1372
largest diff peak and hole, $\text{e}\cdot\text{\AA}^{-3}$	2.1 and -1.6	0.5 and -0.8	0.7 and -0.5	1.3 and -1.0
CCDC number	263803	263804	263805	263806

of an electronically integrating actinometry device,¹⁰⁰ which provides a numerical value for the total amount of light absorbed by the system, $\int_0^t Q_{\text{abs}} dt$ (einstein L^{-1}), and thus eliminates any problems arising from nonconstant photon fluxes and/or incomplete absorption of light in the sample cell. The instrument was calibrated by ferrioxalate actinometry.^{101,102} Irradiation at 365 and 313 nm, respectively, of 3.0 mL aliquots of stock solutions of $\text{W}(\text{CO})_6$ (1 mM) in *n*-hexane containing bis(trimethylsilyl)ethyne (20 mM) was carried out at $25 \pm 1^\circ\text{C}$ in quartz cuvettes (*d* = 1 cm) by using a Hanovia 1000 W Hg–Xe lamp connected to a Schoeffel Instruments GM 252 grating monochromator. The light intensities were on the order of 1.6×10^{-6} and 1.8×10^{-6} einstein·min^{−1} absorbed by the 3.0 mL samples at 365 and 313 nm, respectively.

Quantitative IR spectroscopy (Bruker IFS 66 spectrometer operating with 0.5 cm^{−1} resolution; IR cell with CaF_2 windows, *d* = 203.8 μm) was employed to determine the concentrations of $\text{W}(\text{CO})_6$ (ϵ = 73 430 $\text{L}\cdot\text{mol}^{-1}\cdot\text{cm}^{-1}$ at 1983.3 cm^{−1}) and $\text{W}(\text{CO})_5(\eta^2\text{-btmse})$ (**1**, ϵ = 22 390 $\text{L}\cdot\text{mol}^{-1}\cdot\text{cm}^{-1}$ at 1953.0 cm^{−1}). The following UV–vis molar absorbance data were used to account for mutual internal light filtering. $\text{W}(\text{CO})_6$: ϵ = 303 $\text{L}\cdot\text{mol}^{-1}\cdot\text{cm}^{-1}$ (at 365 nm) and 2670 $\text{L}\cdot\text{mol}^{-1}\cdot\text{cm}^{-1}$ (at 313 nm). **1**: ϵ = 1560 $\text{L}\cdot\text{mol}^{-1}\cdot\text{cm}^{-1}$ (at 365 nm) and 7530 $\text{L}\cdot\text{mol}^{-1}\cdot\text{cm}^{-1}$ (at 313 nm).

X-ray Diffraction Structure Analyses. Crystals of **1** (grown from *n*-hexane), **2**, **3**, and **4** (grown from *n*-pentane) were mounted in glass capillaries (**1**, **4**) or fixed on glass fibers using perfluoropolyether oil (**2**, **3**). Intensity data were collected

on Enraf-Nonius CAD-4 (**1**), Bruker-Nonius KappaCCD (**2**), and Siemens SMART (**3**, **4**) diffractometers. Details of the crystal data and structure analyses are given in Table 6. The structures were solved by the heavy atom method (SHELXS-97).¹⁰³ Refinement was by full matrix least-squares methods (SHELXL-97),¹⁰⁴ where the function $\sum w(F_o^2 - F_c^2)^2$ was minimized. H atom positions were found and included but constrained in the final refinement stage for all compounds. DIAMOND drawings¹⁰⁵ of the molecular structures are displayed in Figure 2 (complexes **1–3**) and Figure 5 (complex **4**), and selected bond distances and angles are collectively listed in Table 1 (complexes **1–3**) and Table 4 (complex **4**).

Acknowledgment. The authors wish to thank P. Bayer and D. Merkl for skillful technical assistance. Financial Support (to S.Ö.) by the Alexander von Humboldt Stiftung and the Turkish Academy of Sciences is gratefully acknowledged.

Supporting Information Available: IR spectra of $\text{Mo}(\text{CO})_5(\eta^2\text{-btmse})$ (**2**) and $\text{Cr}(\text{CO})_5(\eta^2\text{-btmse})$ (**3**) in the $\nu(\text{CO})$ region. Tables of bond lengths and angles, atomic coordinates, and thermal parameters for $\text{W}(\text{CO})_5(\eta^2\text{-btmse})$ (**1**), $\text{Mo}(\text{CO})_5(\eta^2\text{-btmse})$ (**2**), $\text{Cr}(\text{CO})_5(\eta^2\text{-btmse})$ (**3**), and *trans*- $\text{Mo}(\text{CO})_4(\eta^2\text{-btmse})_2$ (**4**). Structures of the two crystallographically independent molecules per asymmetric unit in the crystal of **2** and **4**. This material is available free of charge via the Internet at <http://pubs.acs.org>.

OM058016R

(100) Amrein, W.; Gloor, J.; Schaffner, K. *Chimia* **1974**, *28*, 185–188.

(101) Hatchard, G. G.; Parker, C. A. *Proc. R. Soc. London, A* **1956**, *235*, 518–536.

(102) Murov, S. L. *Handbook of Photochemistry*; Dekker: New York, 1973; p 119.

(103) SHELXS-97: Sheldrick, G. M. *Acta Crystallogr. A* **1990**, *46*, 467–473.

(104) Sheldrick, G. M. SHELXL-97, Program for crystal structure refinement; University of Göttingen: Germany, 1997.

(105) DIAMOND, Version 2.1c; Crystal Impact GbR: Bonn, Germany, 1999.